Underexposed Image Correction Via Approximation of the Scene Radiance Function

Antonio Robles-Kelly and Edwin R. Hancock
Department of Computer Science,
University of York,York YO1 5DD, UK.
{arobkell,erh}@cs.york.ac.uk

Abstract

In this paper, we describe a method for correcting underexposed images by recovering the Lambertian diffuse component in the scene. The method makes use of an implicit mapping between the objects in the scene and a unit sphere. As a result of this treatment, the scene radiance function can be represented by a polar function on the unit sphere. We pose the problem of recovering the scene radiance function as that of estimating a tabular representation of this polar function. We demonstrate how image gradient information can be used to perform the required mapping. With the mapping at hand, we generate an image corresponding to the diffuse component of the scene. The diffuse and input images are then blended in order to obtain the corrected image. We present results on images of real-world scenes and provide comparison with an alternative.

1. Introduction

The modeling of surface reflectance is a topic that is of pivotal importance, and has hence attracted considerable effort in both, computer vision and computer graphics communities. When the reflectance distribution function of the objects in the scene is at hand, then a number of image analysis tasks may be addressed. For instance, Nayar and Bolle [1] have used photometric invariants derived from the reflectance function to recognise objects with different reflectance properties. In a related development, Dror *et al.* [2] have shown how surfaces may be classified from single images through the use of reflectance properties.

Broadly speaking, the methods used to model or approximate the bidirectional reflectance distribution function (BRDF) can be divided into those that are physics-based, semi-empirical or empirical in nature. Although the literature from physics is vast, it is perhaps the work of Beckmann on smooth and rough surface reflectance that is the best known in the vision and graphics communities [3]. Despite being based upon physically meaningful surface parameters, the Beckmann theory is intractable for analysis problems since it relies on the evaluation of the Kirchhoff wave scattering integral. Further, it breaks down when either the surface roughness or the scattering angle are large. However, recently, Vernold and Harvey [4] have overcome this latter problem by developing a model which accounts for self shadowing on rough surfaces. By contrast, in the graphics community it is the development of computationally efficient tools for the purposes of realistic surface rendering that is of primary interest, and hence it is empirical models that have been the focus of activity. One of the most popular models is that developed by Phong

BMVC 2004 doi:10.5244/C.18.58

[5]. However, neither the models developed in physics nor the computational models developed in graphics are well suited for surface analysis tasks in computer vision. It is for this reason that Wolff [6] and Nayar and Oren [7] have developed phenomenological, or semi-empirical, models that account for departures from Lambertian reflectance.

An alternative is to empirically estimate or to learn the BRDF under controlled lighting and viewing conditions of rough and specular objects [8, 9, 10, 11]. There have also been attempts to model the reflectance properties of human skin from real-wold imagery [12, 13]. Hertzmann and Seitz [14] have shown how the BRDF can be recovered making use of a reference object and multiple views of the scene.

The main problem with existing approaches is that the BRDF has four degrees of freedom, which correspond to the zenith and azimuth angles for the light source and the viewer relative to the surface normal direction. As a result, the tabulation of empirical BRDF's can be slow and labour intensive. Furthermore, extensive lighting control and prior knowledge of the surface geometry is often required for the BRDF estimation process. There are a number of ways in which reflectance can depart from the Lambertian case. There have been several attempts to remove specularities from images of non-Lambertian objects. For instance, Brelstaff and Blake use a simple thresholding strategy to identify specularities on moving curved objects [15]. Ragheb and Hancock [16] have developed a probabilistic framework for specularity subtraction which uses the Torrance and Sparrow model to account for the distribution of image brightness. The main limitation of these methods is that they rely on the use of the BRDF to characterise the specular spike and lobe. As a result, they lack the generality required to process real-world imagery in an unsupervised or automatic way.

In this paper, we build upon the fact that the radiance of a scene can be decomposed into reflectance and illumination components [17] and, hence, the exposure of images whose scene is predominantly specular may be corrected making use of the reflectance distribution function. To approximate the reflectance function, we commence by developing an essentially non-parametric method for estimating the reflectance function for the objects in the scene from image data. Here, we avoid using basis functions or a predetermined reflectance function to characterise the specular spike and limb. Our method makes implicit use of the Gauss map, i.e. the projections of the surface normals onto a unit sphere. By making use of differential geometry, we show how the reflectance function can be represented by a polar function on the unit sphere. We pose the problem of recovering the reflectance function as that of estimating a tabular representation of this polar function. A simple analysis shows how this tabular representation of the reflectance function can be obtained using the cumulative distribution of image gradients. We show how the scene radiance function delivered by our method can be used to recover an image whose diffuse component is dominant. The corrected image is the product of the blending of this diffuse image and the one provided at input.

2. Prerequisites

Our starting point in this paper is the assumption that the lighting in the scene can be decomposed into a specular and a diffuse component. Recall that specular highlights are areas of high reflectivity in the scene. As a result, underexposure preserves better specular reflectance and diffuse reflectance becomes a small contribution to the overall lighting conditions captured in the image. This contributes to the image appearing "dark"

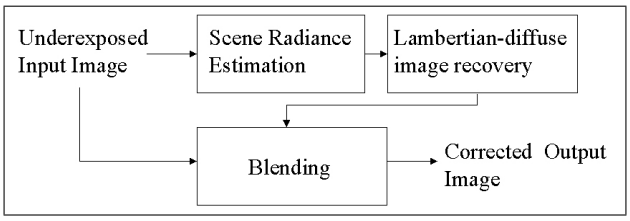

Figure 1: Diagrammatic representation of the exposure correction process.

to the viewer. Following this rationale, we correct this problem by recovering an image in which the specularities have been removed. This image, which represents the diffuse component, is then blended with the underexposed image in order to obtain the corrected image delivered at output by our algorithm. A diagram of this procedure is shown in Figure 1.

As mentioned earlier, our first step in the correction process is to recover the average reflectance function for the objects in the image. To do this, we model the scene as a single object and recover the reflectance function for the corresponding surface. We also consider the surface $S \in \Re^3$, corresponding to the scene, as being illuminated from a direction $\vec{L}$ equal to the viewer's direction $\vec{V}$. Further, we model its reflectance as being isotropic and monotonic. The reasons why we can do this are twofold. First, since we aim to recover the diffuse component of the same surface S illuminated from the same direction and viewed from the same point in space, no inconsistencies in re-illumination or pose arise by assuming $\vec{L} = \vec{V}$ when the diffuse component is recovered. Second, the mathematical conditions introduced during the development of the reflectance function recovery process presented in this paper imply that the image gradient magnitude for a particular brightness value is in average the same on an "arbitrary" surface S. As a result, due to the fact that the surface S remains constant throughout the process, the recovered diffuse image is consistent with the input image. This, in turn, allows the blending to be performed.

3. Scene Radiance Estimation

In this section, we provide the background for our method. Our overall aim is to make an estimate of the reflectance distribution from a single image of the scene. To commence, consider the scene as an illuminated surface denoted by $S \in \Re^3$. At this point, it is worth noting that the process developed in this and the next sections is applied identically for the three RGB colour-channels comprising the image. Hence, in practice, we will be taking as the input to our method a set of three single-brightness images of the surface S formed on the image plane Π. Each of these singe-brightness images correspond to one of the three colour-channels.

The geometry of the reflectance process can be expressed in terms of unit vectors in the directions of the surface normal, the viewer direction and the light-source direction. The light-source $\vec{L}$, viewer $\vec{V}$ and surface normal $\vec{N}$ vectors respectively have elevation and azimuth angles (θ_L, α_L), (θ_V, α_L) and (θ_N, α_N). We use the surface normal vector $\vec{N}$ as a reference and define the following elevation and azimuth angle offsets for the light-source and viewer directions $\alpha_i = \alpha_N - \alpha_L$, $\alpha_r = \alpha_N - \alpha_V$, $\theta_i = \theta_N - \theta_L$ and $\theta_r = \theta_N - \theta_V$.

Suppose that the irradiance incident at the point s on the surface is $f_I(\theta_i, \alpha_i)$. The outgoing radiance from the point s is $f_O(\theta_r, \alpha_r)$. The bidirectional reflectance distribution function (BRDF) is defined to be the ratio of the emitted surface radiance to the incident irradiance, i.e.

$$\rho(\theta_i, \alpha_i, \theta_r, \alpha_r) = \frac{f_O(\theta_r, \alpha_r)}{f_I(\theta_i, \alpha_i)\cos(\theta_i)d\omega} \tag{1}$$

As noted earlier, since there are no transformations to the surface S throughout the exposure correction process, we can confine our attention to the case where the light-source direction is fixed to be the same as that of the viewer. Hence, the angles of incidence and emission are equal to the angle subtended by the surface normal to the viewer/light-source direction. Hence, $\theta = \theta_i = \theta_r$ and $\alpha = \alpha_i = \alpha_r$. Under these conditions, the angular dependance of the BRDF is determined just by the direction of the surface normal. Moreover, we assume that the light-source is a point at infinity, and hence the irradiance is constant, i.e. $f_I(\theta, \alpha) = k$. Hence, we can write $\rho(\theta, \alpha) = k\frac{f_O(\theta,\alpha)}{\cos(\theta)d\omega}$. Furthermore, if we assume that the image is formed by orthographic projection of the surface, then the measured image brightness is proportional to $f_O(\theta, \alpha) = \frac{1}{k}\rho(\theta, \alpha)\cos(\theta)$. Hence, the problem reduces to that of providing a means of estimating the radiance function $f_O(\theta, \alpha)$ from single images of surfaces illuminated under conditions in which the light-source and viewer directions are identical.

We simplify the problem of estimating the radiance function by exploiting differential geometry and making use of the Gauss map from the surface onto a unit sphere. For an orientable surface $S \in \Re^3$, the Gauss map $G : S \mapsto \hat{S}$ maps points on the surface S onto locations on the unit sphere $\hat{S}$ which have identical surface normal directions. Our aim is to use correspondences between surface normal directions to map brightness values from the image onto the unit sphere. The polar distribution of brightness on the unit sphere $\hat{S}$ is the radiance function for the surface. To avoid ambiguities, we assume that points on the surface with identical surface normals have identical brightness values.

Of course, in practice we do not have surface normals to hand and hence the mapping of the brightness values from the image onto the unit-sphere is not straightforward. Hence, we specialise our discussion to the case where the plane Π is chosen so that the viewer direction $\vec{V}$ and the light-source direction $\vec{L}$ vectors are co-incident, i.e. $\vec{L} = \vec{V}$. Suppose that the point p on the unit sphere has zenith angle θ and azimuth angle α. Under the Gauss map, the brightness value associated with this point is denoted by the polar radiance function $f_O(\theta, \alpha) = I$, where I is the measured brightness at the corresponding point s in the image of the surface S. As noted above, when $\vec{L} = \vec{V}$, then provided that the reflectance process is isotropic, then the distribution of radiance across the unit sphere can be represented by a function $g(\theta)$ of the zenith angle alone. As a result, the observed brightness values mapped onto the unit sphere by the Gauss map G can be generated by revolving the function $g(\theta) = f_O(\theta, 0)$ in azimuth angle α about the axis defined by $\vec{L}$ and $\vec{V}$. The problem of describing the observed brightness distribution over the Gauss sphere hence reduces to that of approximating the function $g(\theta)$ and computing its trace of revolution.

When $\vec{L} = \vec{V}$, as noted earlier, the task of estimating the radiance function reduces to that of estimating the distribution of brightness with zenith angle on the unit sphere, i.e to estimating $g(\theta)$. We show how this can be performed by using the differential structure of the observed brightness on the image plane Π. Hence, we commence rewriting $g(\theta)$ as the integral of the partial derivative of the observed brightness with respect to the angular

variable θ. To do this, we assume the radiance function $f_O(\theta,\alpha)$ to be monotonically decreasing and write

$$g(\theta) = \frac{1}{2\pi}\int_0^{2\pi}\left(f_O(0,\alpha) + \int_0^{\theta}\frac{\partial f_O(\theta,\alpha)}{\partial\theta}d\theta\right)d\alpha \tag{2}$$

In other words, the generating function $g(.)$ on the unit sphere can be expressed in term of the cumulative distribution of the derivatives of the radiance function or alternatively the derivatives of the image brightness.

Consider the image of the unit sphere on the plane Π. Suppose that $F(r,\theta)$ is a parametric polar function that represents the distribution of radiance over the image of the unit sphere. The radial component of this function can be used to approximate the generator of the radiance function on the unit sphere $\hat{S}$, i.e. $g(\theta)$. The radial coordinate of the function is the Euclidean distance between the point p and the center-point of the unit sphere $\hat{S}$ on the viewer plane $\hat{\Pi}$, i.e. $r = \sqrt{(\sin(\theta)\cos(\alpha))^2 + (\sin(\theta)\sin(\alpha))^2} = \sin(\theta)$. Hence

$$F(r,\theta) = \begin{bmatrix} r \\ g(\theta) \end{bmatrix} = \begin{bmatrix} \sin(\theta) \\ \frac{1}{2\pi}\int_0^{2\pi}\left(f_O(0,\alpha) + \int_0^{\theta_p}\frac{\partial f_O(\theta,\alpha)}{\partial\theta}d\theta\right)d\alpha \end{bmatrix} \tag{3}$$

Since the surface normals are not at hand, the correspondences between locations on the surface and the unit sphere are not available. Hence, the quantity θ is unknown. In other words, the function $F(r,\theta)$ only allows the surface S to be mapped onto the unit sphere $\hat{S}$ in an implicit manner.

Using the Jacobian for the transformation between the image plane and the unit sphere, it is a straightforward matter to show that

$$|\nabla I| = \frac{1}{\cos(\theta)}\frac{\partial g(\theta)}{\partial\theta} = \frac{\partial g(\theta)}{\partial\sin(\theta)} \tag{4}$$

In this way, we can relate the image gradient to the derivative of the function $g(\theta)$ with respect to the zenith angle θ. In terms of finite differences, the relationship between the image gradient and the changes $\Delta g(\theta)$ in $g(\theta_p)$ and $\Delta\sin(\theta)$ in θ is the gradient of the function $F(r,\theta)$, i.e. $|\nabla I| = [\Delta g(\theta)]/[\Delta\sin(\theta)]$.

The image gradient can be computed using the formula

$$\nabla I = \frac{1}{\delta}\begin{bmatrix} I(j+1,k) - I(j-1,k) \\ I(j,k+1) - I(j,k-1) \end{bmatrix} \tag{5}$$

where δ is the spacing of sites on the pixel lattice. Furthermore, on the unit sphere $\hat{S}$, it is always possible to choose points to be sampled so that the difference in brightness is a constant τ. As a result, we can write $\Delta\sin(\theta) = \tau/|\nabla I|$.

To recover θ from the expression above we perform numerical integration. To do this, we sort the image gradients according to the associated image brightness values. Accordingly, let ∇I_l be the image gradient associated with the brightness value l. The numerical estimate of $\sin(\theta)$ is found by summing or integrating the distribution of gradients over brightness

$$\sin(\theta) = \sum_{l=0}^{m}\frac{\tau}{|\nabla I_l|} + \kappa \tag{6}$$

where κ is the integration constant and m is the maximum brightness value. Hence, we can use the cumulative distribution of inverse gradients to index the zenith angle on the unit sphere. This indexation property means that we can approximate the function $F(r,\theta)$ or equivalently $g(\theta)$ by tabulation.

To pursue this idea, in principle, we only require a single image gradient corresponding to each of the distinct brightness levels in the image. In practice, we make use of the cumulative distribution of image gradients in order to minimise the approximation error by averaging. Let $H(l) = \{s \mid I = l\}$ be the set of pixels with brightness value l. For the brightness value $l = g(\theta)$, the average gradient is given by

$$h(l) = \frac{\sum_{s \in H(l)} \mid \nabla I \mid}{\mid H(l) \mid} \tag{7}$$

The distribution of average gradient over brightness is stored as a vector h. Zero entries of the vector, which correspond to brightness values that are not sampled in the image, can cause divide-by-zero errors when the radiance function is computed. To overcome this problem, we smooth the components of the vector by performing piecewise linear interpolation of the adjacent non-zero elements. The resulting vector is denoted by $\hat{h}$. With the average image gradient to hand, we define the tabular approximation $\hat{F}$ to $F(r,\theta)$ as the set of Cartesian pairs

$$\hat{F} = \{((\tau \sum_{i=0}^{l} \hat{h}(l)^{-1} + \kappa), l); l = 0,1,2,\ldots,n_{max}\} \tag{8}$$

where n_{max} is the maximum brightness value in the image. All that remains is to compute the constants τ and κ. We do this by making use of the maximum and minimum values of $\sin(\theta)$. Since the maximum and minimum values of $\sin(\theta)$ are unity and zero when $\theta = \pi/2$ and $\theta = 0$, we can set κ to unity. Evaluating the numerical integral for $l = m$ (i. e. $\sin(0) = 0$), we get

$$\tau = -\left(\sum_{i=0}^{m} \hat{h}(i)^{-1}\right)^{-1} \tag{9}$$

4. Diffuse Component Recovery

In this section, we show how the tabular representation of the function $\hat{F}$ recovered in the previous section may be used for re-mapping a Lambertian reflectance model onto the input image. We use this re-mapping to both remove specularities from the input image and to correct for reduced boundary contrast resultant of poor illumination conditions.

The idea underpinning this procedure is to re-map the image brightness using the inverse Gauss mapping from the unit sphere onto the original image. To do this, we center our attention in a simple Lambertian reflectance model.

Stated formally, our aim is to use the tabular representation of the function $\hat{F}$ to retrieve the Lambertian radiance at a given point on the surface S illuminated from a light source with direction vector $[0,0,1]^T$. To do this we note that the tabular function $\hat{F}$ is a list of Cartesian pairs in which the first element is the sine of the elevation angle of the surface normals, i.e. $\sin(\theta)$ while the second element is the associated image brightness, i.e. at a point indexed s on the surface S. For Lambertian reflectance, the observed radiance is proportional to the cosine of the angle of light incidence, i.e. to $\cos(\theta)$. Hence,

we can perform Lambertian re-illumination by noting the observed brightness at a pixel p and identifying the associated value of $\sin(\theta)$. The corresponding corrected Lambertian radiance is $\cos(\theta)$.

The radiance re-mapping can be effected using the measured image gradient. Suppose that $\mathscr{R}$ is a neighbourhood with area $\mathscr{A}$ centered at the pixel location indexed p. We compute the corrected Lambertian radiance by averaging $\cos(\theta)$ over the neighbourhood $\mathscr{R}$. Since the angle θ is defined on the unit sphere, while the brightness is required on the image plane, we weight the average using the $\cos(\theta)$ and write

$$\hat{I} = \frac{\int_{\mathscr{A}} \cos(\theta) \frac{\partial g(\theta)}{\partial \sin\theta} d\mathscr{A}}{\int_{\mathscr{A}} \frac{\partial g(\theta)}{\partial \sin\theta} d\mathscr{A}} \tag{10}$$

From the analysis presented in the preceding section it follows that the quantity $\cos(\theta)$ is proportional to the image gradient. Making the substitution $|\nabla I| = \frac{\partial g(\theta)}{\partial \sin\theta}$, we find that the discrete approximation to the corrected Lambertian radiance at a pixel p with coordinates u on the image plane is given by

$$\hat{I}(u) = \frac{1}{\mu} \sum_{q \in \mathscr{R}} \left\{ \cos(\theta) \mid \nabla I(v) \mid \right\} \tag{11}$$

where $\mid \nabla I(v) \mid$ is the magnitude of the image intensity gradient at the pixel-site indexed q, whose coordinates are $v = (j,k)$ and

$$\mu = \sum_{q \in \mathscr{R}} \mid \nabla I(v) \mid \tag{12}$$

is the average image gradient. We approximate the cosine of θ making use of the average image brightness gradient as follows

$$\cos(\theta) \approx \cos\left(\arcsin\left(\tau \sum_{i=0}^{I(u)} \hat{h}(i)^{-1} + \kappa \right) \right) \tag{13}$$

This averaging process effectively smooths the estimate of the Lambertian radiance.

5. Image Blending

Once the input and the diffuse images are to hand, we proceed to combine them via a simple blending operation. This blending operation effectively averages the brightness values I and $\hat{I}$ each pixel-site in the image. The idea underpinning this procedure stems from the fact that, as mentioned earlier, underexposure can be considered to be the result of areas of high reflectivity in the scene. The input image can then be viewed as one in which the specular component is dominant while the image recovered by our algorithm can be regarded as one in which the diffuse component is larger. Hence, the blending of both gives at output an image that is the linear combination of the specular and diffuse components in the scene.

6. Experiments

We have experimented with a variety of images from real-world scenery. Here, we present results for four underexposed images acquired under a variety of lighting conditions.

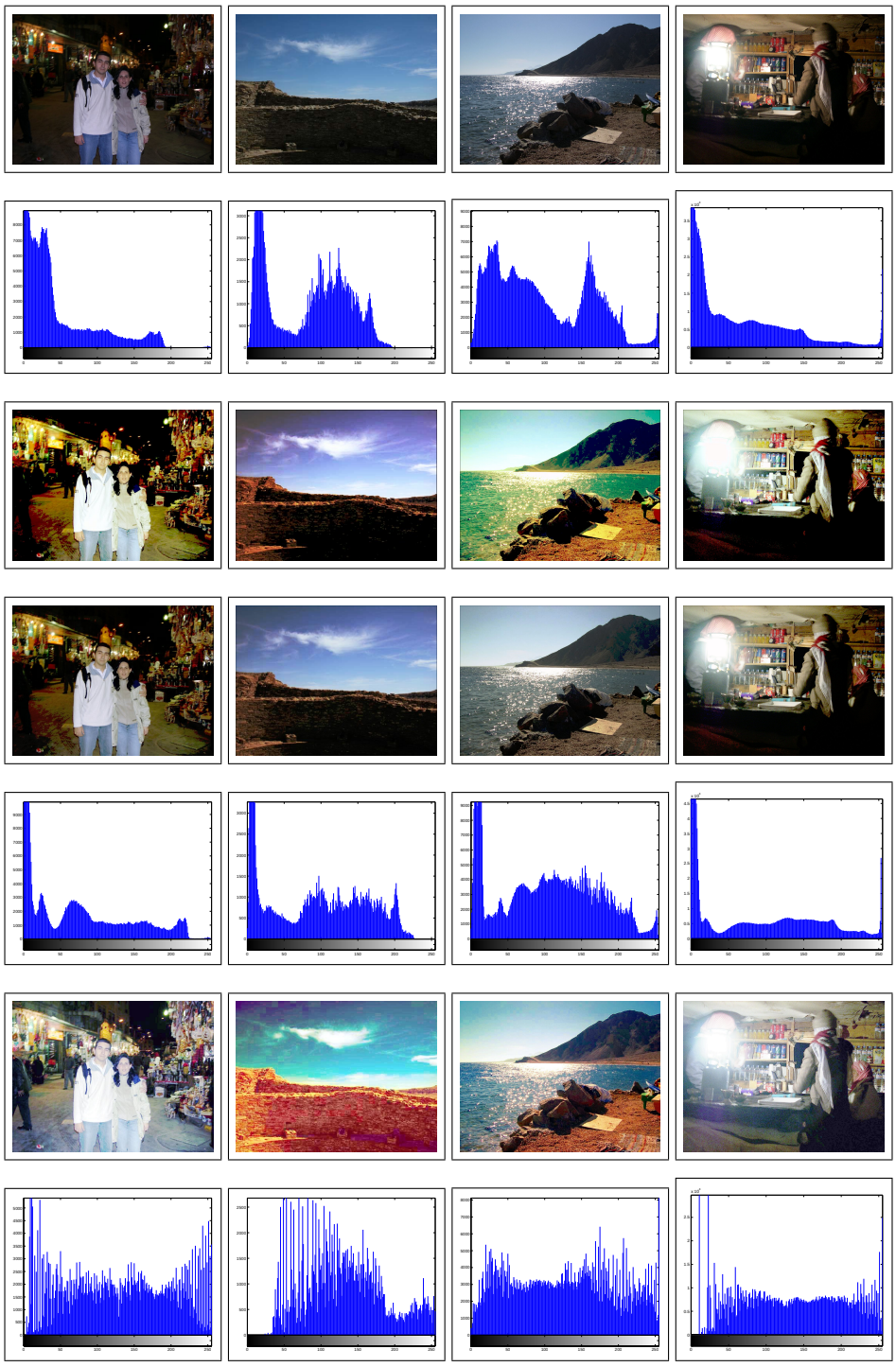

Figure 2: From top-to-bottom: Underexposed input images; Brightness histograms for the input images; Lambertian-diffuse image recovered using our algorithm; Output image (blending of the input image and the Lambertian-diffuse image); Brightness histogram for the output images; Results of the equalisation using CLAHE; Brightness histogram for the images equalised via CLAHE.

These are a picture of a scene in a market acquired in nocturnal conditions, two landscape pictures acquired in strong sunlight and a picture acquired indoors. To acquire these images we used a Nikon Coolpix 4300 digital camera. All our images were acquired using the default settings for true-color, 4 Mpixel pictures. We show our input images in the top row of Figure 2. The second row, we show the brightness histograms for each of the input images. In the third row, we show the diffuse images recovered using our method. From the experiments, its clear that the algorithm has removed the specularities in the input image reasonably well. It is also clear that a lot of background detail becomes visible when the "flattening", due to the specular spike and limb, is removed from the scene. Moreover, in contrast with the input image, the diffuse images appear to be artificially "bright". This is particularly visible in the picture of the seaside landscape and the market image. The reason for this is that, in practice, purely diffuse scenes are difficult to find and so the images delivered by this step of our algorithm present an unusual lightness and hue. In the fourth row, we show the blending results for each of the input images. In our experiments, we have used a blending opacity of 50%. In contrast with the input and diffuse images, the blended images capture the detail of the scene while presenting better contrast. Moreover, the levels of hue and brightness have been greatly improved. The fifth row shows the image intensity histogram for the corrected images.

In the sixth row of Figure 2 we show the results delivered by contrast-limited histogram equalization (CLAHE) [18]. This is an image processing technique that hinges in dividing the image into regions whose intensity histogram is required to approximate, at output, a predetermined distribution. Our implementation of CLAHE makes use of 16 by 16 pixel regions, a uniform distribution and the adaptive contrast enhancement algorithm of Stark [19] as a preprocessing step. It is worth stressing that the algorithm of Stark is a routine built into the CLAHE implementation and, therefore, has not been used in our correction method. The image intensity histograms for the images equalised via CLAHE are shown in the bottom row.

In contrast with the results delivered by our method, the images enhanced using CLAHE show biasing of the image brightness towards the extrema. The effect of this is that the images appear to be "opaque" or "foggy". Further, from the histograms, becomes evident that our method has preserved the shape of the initial distribution of image brightness while improving the contrast.

7 Conclusions

In this paper, we have presented a method for correcting underexposed images that involves recovering the diffuse component for the input image. In order to recover the Lambertian-diffuse component, we make use of an implicit mapping between the objects in the scene and a unit sphere. As a result of this treatment, the scene radiance can be estimated using a a tabular representation of a polar function on the unit sphere. With this tabular representation to hand, we generate an image that corresponds to the Lambertian-diffuse component of the scene. Both, the input and diffuse, images are then blended to obtain the corrected image. From our experiments, we can conclude that the corrected images reproduce well the detail of the input images while showing better contrast and levels of hue and brightness.

References

[1] S. Nayar and R. Bolle, "Reflectance based object recognition," *International Journal of Computer Vision*, vol. 17, no. 3, pp. 219–240, 1996.

[2] R. O. Dror, E. H. Adelson, and A. S. Willsky, "Recognition of surface reflectance properties from a single image under unknown real-world illumination," in *Proc. of the IEEE Workshop on Identifying Objects Across Variations in Lighting*, 2001.

[3] P. Beckmann and A. Spizzochino, *The Scattering of Electromagnetic Waves from Rough Surfaces*, Pergamon, New York, 1963.

[4] C. L. Vernold and J. E. Harvey, "A modified beckmann-kirchoff scattering theory for non-paraxial angles," in *Scattering and Surface Roughness*, 1998, number 3426 in Proc. of the SPIE, pp. 51–56.

[5] B. T. Phong, "Illumination for computer generated pictures," *Communications of the ACM*, vol. 18, no. 6, pp. 311–317, 1975.

[6] L. B. Wolff, "On the relative brightness of specular and diffuse reflection," in *Int. Conf. on Comp. Vision and Patt. Recognition*, 1994, pp. 369–376.

[7] S. K. Nayar and M. Oren, "Visual appearance of matte surfaces," *SCIENCE*, vol. 267, pp. 1153–1156, 1995.

[8] S. Westin, J. Arvo, and K. Torrance, "Predicting reflectance functions from complex surfaces," in *SIGGRAPH 92 Conference Proceedings*, 1992, pp. 255–264.

[9] G. J. Ward, "Measuring and modeling anisotropic reflection," *Computer Graphics*, vol. 26, no. 2, pp. 265–272, 1992.

[10] E. P.F. Lafortune, Sing-Choong Foo, K. E. Torrance, and D. P. Greenberg, "Non-linear approximation of reflectance functions," in *SIGGRAPH 97 Conference Proceedings*, 1997, pp. 117–126.

[11] K. J. Dana and S. K. Nayar, "Correlation model for 3d texture," in *Int. Conf. on Comp. Vision*, 1999, pp. 1061–1066.

[12] S. R. Marschner, S. H. Westin, E. P. F. Lafortune, K. E. Torrance, and D. P. Greenberg, "Image-based brdf measurement including human skin," in *10th Eurographics Rendering Workshop*, 1999.

[13] P. Debevec, T. Hawkins, C. Tchou, H.-P. Duiker, W. Sarokin, and M. Sagar, "Acquiring the reflectance field of a human face," in *SIGGRAPH 2000*, 2000, pp. 145–156.

[14] A. Hertzmann and S. M. Seitz, "Shape and materials by example: A photometric stereo approach," in *Int. Conf. on Comp. Vision and Patt. Recognition*, 2003, pp. 533–540.

[15] G. Brelstaff and A. Blake, "Detecting specular reflection using lambertian constraints," in *Int. Conf. on Comp. Vision*, 1988, pp. 297–302.

[16] H. Ragheb and E. R. Hancock, "A probabilistic framework for specular shape-from-shading," *Pattern Recognition*, vol. 36, no. 2, pp. 407–427, 2003.

[17] H. G. Adelmann, "Butterworth equations for homomorphic filtering of images," *Computers in Biology and Medicine*, vol. 28, pp. 169–181, 1998.

[18] K. Zuiderveld, *Contrast Limited Adaptive Histogram Equalization*, chapter Graphics Gems IV, pp. 474–485, Academic Press, 1994.

[19] J. A. Stark, "Adaptive image contrast enhancement using generalizations of histogram equalization," *IEEE Trans. on Image Processing*, vol. 9, no. 5, pp. 889–896, 2000.